

Synthesis, Reactivity, and Computational Studies of $[\eta^5\text{-C}_5\text{H}_5\text{-(}\eta^5\text{-C}_5\text{H}_4\text{CMe}_2\text{C}_6\text{H}_4\text{Me)TiMe}]^+$: Aromatic C–H Bond Activation at $-50\text{ }^\circ\text{C}^\S$

Jörg Sassmannshausen*[†] and Judith Baumgartner[‡]

Institute for Chemistry and Technology of Organic Materials, TU-Graz, Stremayrgasse 16/I A-8010 Graz, Austria, and Inorganic Chemistry, TU-Graz, Stremayrgasse 16/I A-8010 Graz, Austria

Received January 15, 2008

The titanocene compound $[\eta^5\text{-C}_5\text{H}_5\text{-(}\eta^5\text{-C}_5\text{H}_4\text{CMe}_2\text{C}_6\text{H}_4\text{Me)TiMe}]$ (**1**) was prepared from the titanocene dichloride precursor $[\eta^5\text{-C}_5\text{H}_5\text{-(}\eta^5\text{-C}_5\text{H}_4\text{CMe}_2\text{C}_6\text{H}_4\text{Me)TiCl}_2]$ (**1a**). The solid-state structures of **1a** and **1** were determined and are similar to other titanocene compounds. The reaction of compound **1** with $\text{B}(\text{C}_6\text{F}_5)_3$ in CD_2Cl_2 was monitored by NMR spectroscopy. At $-60\text{ }^\circ\text{C}$ the expected cationic compound $[\eta^5\text{-C}_5\text{H}_5\text{-(}\eta^5\text{-C}_5\text{H}_4\text{CMe}_2\text{C}_6\text{H}_4\text{Me)TiMe}]^+$ (**2**) with a coordinated tolyl group was observed. Warming the samples to $-50\text{ }^\circ\text{C}$ leads to evolution of methane, indicating C–H bond activation of the coordinated tolyl moiety. The so-formed titanacycles form with the anion $[\text{MeB}(\text{C}_6\text{F}_5)_3]^-$ the inner sphere ion pair (ISIP) $[\eta^5\text{-C}_5\text{H}_5\text{-(}\eta^5\text{-}\sigma^1\text{-C}_5\text{H}_4\text{CMe}_2\text{C}_6\text{H}_3\text{Me)Ti-}\mu\text{-MeB}(\text{C}_6\text{F}_5)_3]$ (**3**) and is in exchange with an outer sphere ion pair $[\eta^5\text{-C}_5\text{H}_5\text{-(}\eta^5\text{-}\sigma^1\text{-C}_5\text{H}_4\text{CMe}_2\text{C}_6\text{H}_3\text{Me)Ti}]^+[\text{MeB}(\text{C}_6\text{F}_5)_3]^-$ (**4**), with the free coordination site probably occupied by a solvent molecule. The structure of **4** could not be determined unambiguously. The homoleptic bimetallic compound $[\{\eta^5\text{-C}_5\text{H}_5\text{-(}\eta^5\text{-C}_5\text{H}_4\text{CMe}_2\text{C}_6\text{H}_4\text{Me)Ti}\}_2\text{-}\mu\text{-Me}]^+$ (**5**) was prepared by reaction of 2 equiv of **1** with 1 equiv of $\text{B}(\text{C}_6\text{F}_5)_3$ in CD_2Cl_2 at $-50\text{ }^\circ\text{C}$ and monitored by NMR spectroscopy. Detailed density functional theory (DFT) studies of the formation of **3** and **4** from **2** corroborate the NMR results.

Introduction

Group 4 metallocene compounds play an important role as catalyst precursors for the hydrogenation,¹ hydrosilylation, and polymerization of olefins.^{2–14} In particular for alkene polymerization, these precursors need to be activated by a *cation-generating compound* (CGA) to form what is believed to be the active species $[\eta\text{-Cp}_2\text{MR}]^+$ (Cp = (substituted) cyclopentadienyl, M = Ti, Zr, Hf). Obviously, this rather “naked” ion does not exist by itself in solution; rather it is paired with a weakly coordinating ligand $[\text{Cp}_2\text{MR}^+\cdots\text{D}]$ (D = X[−] (anion), monomer, solvent). Depending on the concentration, these anion/cation pairs form higher conglomerates like quadruples and

hextuples.¹⁵ Whereas the chemistry of zirconocene compounds appears to be quite predictable, the chemistry of the titanocene compounds is sometimes quite unexpected. For example, some time ago we have reported the formation of *quasi living* polymerization of propene at ambient temperature with the catalytic mixture of $[\eta^5\text{-C}_5\text{Me}_5\text{TiMe}_3]$ with $\text{B}(\text{C}_6\text{F}_5)_3$.^{16,17} Hessen reported the selective *trimerization* of ethene with half-sandwich compounds of titanium with coordinated arene groups.^{18–20} We have recently reported the formation of cationic zirconocene compounds with coordinated arene groups and found that the strength of the coordination strongly depends on the bridging atom of the tether: Whereas a carbon bridge between cyclopentadienyl and arene moieties exclusively gave coordination of the arene to the cationic zirconium, silicon as a bridging atom resulted in a more ambivalent behavior. Here, two different products could be observed: the expected zirconocene cation with a coordinated arene group and the well-known inner sphere ion pair with a zirconium-methyl-boron bridge and a free arene.^{21–26} We reasoned that the coordination

* Corresponding author. E-mail: sassmannshausen@tugraz.at.

[§] Dedicated to F. Stelzer on the occasion of his 60th birthday.

[†] Institute for Chemistry and Technology of Organic Materials.

[‡] Inorganic Chemistry.

(1) Qian, Y.; Li, G.; Huang, Y. *J. Mol. Catal.* **1989**, *54*, L 19.

(2) Bochmann, M.; Cannon, R. D.; Song, F. *Kinet. Catal.* **2006**, *47*, 160–169.

(3) Kaminsky, W. *J. Polym. Sci. A: Polym. Chem.* **2004**, *16*, 3911–3921.

(4) Pedoutour, J.-N.; Radhakrishnan, K.; Cramail, H.; Deffieux, A. *Macromol. Rapid Commun.* **2001**, *22*, 1095–1123.

(5) Bochmann, M. *J. Chem. Soc., Dalton Trans.* **1996**, 255–270.

(6) Bochmann, M. *Top. Catal.* **1999**, *7*, 9–22.

(7) Bochmann, M.; Pindado, G. J.; Lancaster, S. J. *J. Mol. Catal. A: Chem.* **1999**, *146*, 179–190.

(8) Bochmann, M. *J. Organomet. Chem.* **2004**, *689*, 3982–3998.

(9) Brintzinger, H.-H.; Fischer, D.; Mühlhaupt, R.; Rieger, B.; Waymouth, R. *Angew. Chem.* **1995**, *107*, 1255–1383.

(10) Britovsek, G. J. P.; Gibson, V. C.; Wass, D. F. *Angew. Chem., Int. Ed.* **1999**, *38*, 428–447.

(11) Chen, E. Y.-X.; Marks, T. J. *Chem. Rev.* **2000**, *100*, 1391–1434.

(12) Kaminsky, W.; Arndt, M. *Adv. Polym. Sci.* **1995**, *127*, 144–187.

(13) Piers, W. E.; Chivers, T. *Chem. Soc. Rev.* **1997**, *26*, 345–354.

(14) Rempel, G. L.; Huang, J. *Prog. Polym. Sci.* **1995**, *20*, 459–526.

(15) Song, F.; Lancaster, S. J.; Cannon, R. D.; Schormann, M.; Humphrey, S. M.; Zuccaccia, C.; Macchioni, A.; Bochmann, M. *Organometallics* **2005**, *24*, 1315–1328.

(16) Eckstein, A.; Suhm, J.; Friedrich, C.; Maier, R. D.; Sassmannshausen, J.; Bochmann, M.; Mühlhaupt, R. *Macromolecules* **1998**, *31*, 1335–1340.

(17) Sassmannshausen, J.; Bochmann, M.; Rösch, J.; Lige, D. *J. Organomet. Chem.* **1997**, *548*, 23–28.

(18) Deckers, P. J. W.; Linden, A. J. v. d.; Meetsma, A.; Hessen, B. *Eur. J. Inorg. Chem.* **2000**, 929–932.

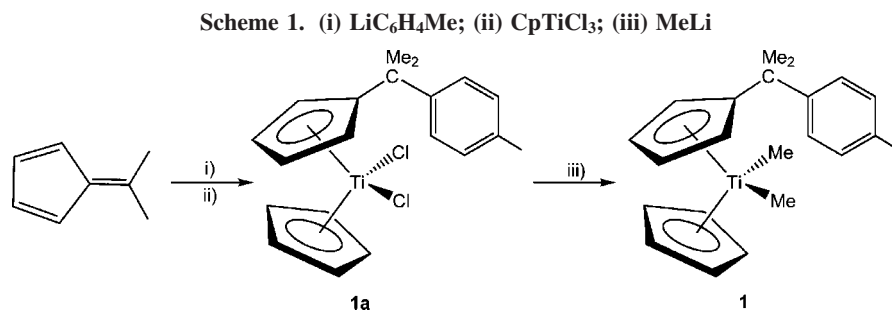
(19) Hessen, B. *J. Mol. Catal. A: Chem.* **2004**, *213*, 129–135.

(20) Otten, E.; Meetsma, A.; Hessen, B. *J. Am. Chem. Soc.* **2007**, *129*, 10100–10101.

(21) Bühl, M.; Sassmannshausen, J. *J. Chem. Soc., Dalton Trans.* **2001**, 79–84.

(22) Doerrer, L. H.; Green, M. L. H.; Häussinger, D.; Sassmannshausen, J. *J. Chem. Soc., Dalton Trans.* **1999**, 2111–2118.

(23) Sassmannshausen, J. *Organometallics* **2000**, *19*, 482–489.



of the arene is strongly susceptible to the steric environment of the metal and thus replaced the metal center with the smaller titanium. We here extend our recent studies on these model systems and report the outcome of detailed NMR and DFT investigations of monosubstituted titanocene compounds of the general type $[\eta^5\text{-Cp-}(\eta^5\text{-C}_5\text{H}_4\text{CMe}_2\text{C}_6\text{H}_4\text{Me})\text{TiMe}]^+$ ($\text{Cp} = \text{C}_5\text{H}_5$). This combination of NMR and DFT investigations has proven to be very successful in the past²¹ and enables investigation of otherwise unobservable reactive intermediates. In Part I, the reaction of **1** with $\text{B}(\text{C}_6\text{F}_5)_3$ in CD_2Cl_2 , investigated by NMR spectroscopy, is discussed. Part II reports the DFT investigation of **2** and the formation of **3** and **4**, respectively.

Results and Discussion

Part I: Preparation of the Metallocenes (1a**, **1**) and Low-Temperature NMR Investigations.** The compounds **1a** and **1** were synthesized according to a modified literature procedure.²² Thus, $\text{LiC}_6\text{H}_4\text{Me}$, freshly prepared from 4-bromotoluene and butyllithium, was reacted with 2,2-dimethylfulvene. The reaction was quenched by addition of $[\eta^5\text{-CpTiCl}_3]$. Recrystallization from toluene yielded crystals of **1a** suitable for X-ray analysis in 62.5% yield. Methylation of **1a** with methyl lithium in toluene yielded **1**. Crystals suitable for X-ray analysis were obtained after recrystallization from pentane in good yield (Scheme 1).

The solid-state structures of **1a** and **1** are depicted in Figures 1 and 2, respectively. Typically for this kind of compound, the arene moiety is pointing away from the titanium in a similar arrangement to the previously published solid-state structure of $[\eta^5\text{-Cp-}\eta^5\text{-(C}_5\text{H}_4\text{CMe}_2\text{C}_6\text{H}_4\text{Me})\text{ZrMe}_2]$.²² Selected bond distances and angles are summarized in Table 1.

Low-Temperature NMR Spectroscopy Reaction Studies. The reaction of **1** with $\text{B}(\text{C}_6\text{F}_5)_3$ in CD_2Cl_2 was monitored by NMR spectroscopy. Similar to the reported compound $[\eta^5\text{-Cp-}(\eta^5\text{-C}_5\text{H}_4\text{CMe}_2\text{C}_6\text{H}_4\text{Me})\text{ZrMe}_2]$, which reacted cleanly at -60°C to form the outer sphere ion pair (OSIP) $[\eta^5\text{-Cp-}(\eta^5\text{-C}_5\text{H}_4\text{CMe}_2\text{C}_6\text{H}_4\text{Me})\text{ZrMe}]^+[\text{MeB}(\text{C}_6\text{F}_5)_3]^-$ as the sole product,²² the observed reaction between **1** and $\text{B}(\text{C}_6\text{F}_5)_3$ yields the OSIP $[\eta^5\text{-C}_5\text{H}_5\text{-}(\eta^5\text{-}\eta^1\text{-C}_5\text{H}_4\text{CMe}_2\text{C}_6\text{H}_4\text{Me})\text{TiMe}]^+[\text{MeB}(\text{C}_6\text{F}_5)_3]^-$ (**2**). Significant are the peaks for the coordinated tolyl moiety, which are observed as doublets at δ (ppm) 7.74, 7.44, 6.77, and 5.78. EXSY (exchange spectroscopy) at this temperature reveals exchange between the *ortho* and *meta* hydrogens, indicating a fluxional coordination of the tolyl moiety to the cationic titanium metal. The four observed signals for the substituted cyclopentadienyl ring together with the two diastereotopic signals for the $-\text{C}(\text{CH}_3)_2$ further corroborate the

suggested structure and agree well with previous results for the zirconocene congener. As expected, the chemical shift of the methyl borate anion δ (ppm) at 0.41 (^1H) and a broad peak at 10 ppm (^{13}C) together with the chemical shift difference $\Delta\delta(\text{m,p})$ of the aryl fluorines of 2.7 ppm are indicative for an

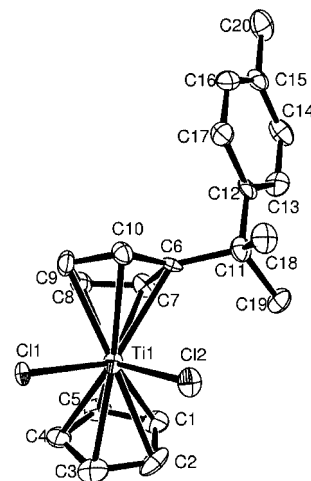


Figure 1. ORTEP representation of **1a**. Ellipsoids are drawn with 50% probability. Hydrogens are omitted for clarity.

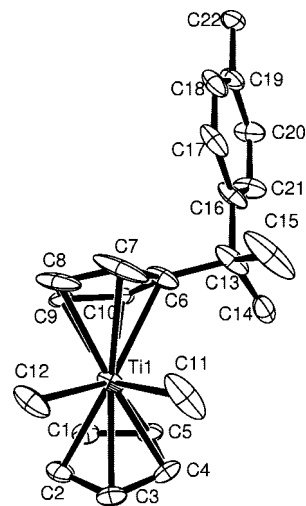


Figure 2. ORTEP representation of **1**. Ellipsoids are drawn with 30% probability. Hydrogens are omitted for clarity.

Table 1. Selected Bond Distances (Å) and Angles (deg) of **1a** and **1**

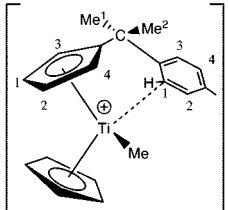
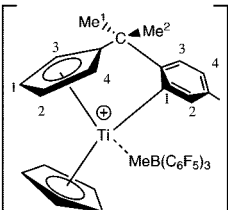
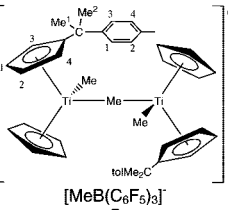
	1a	1	
$d(\text{Ti}-\text{Cl}1)$	2.398(2)	$d(\text{Ti}-\text{Cl}1)$	2.175(5)
$d(\text{Ti}-\text{Cl}2)$	2.354(2)	$d(\text{Ti}-\text{Cl}2)$	2.186(5)
$\angle(\text{Cl}1-\text{Ti}-\text{Cl}2)$	92.15(8)	$\angle(\text{Cl}1-\text{Ti}-\text{Cl}2)$	88.9(2)
$d(\text{Cp}^1_{\text{centr}}-\text{Ti})$	2.063	$d(\text{Cp}^1_{\text{centr}}-\text{Ti})$	2.079
$d(\text{Cp}^2_{\text{centr}}-\text{Ti})$	2.044	$d(\text{Cp}^2_{\text{centr}}-\text{Ti})$	2.059
$\angle(\text{Cp}^1_{\text{centr}}-\text{Ti}-\text{Cp}^2_{\text{centr}})$	131.45	$\angle(\text{Cp}^1_{\text{centr}}-\text{Ti}-\text{Cp}^2_{\text{centr}})$	133.35

(24) Sassmannshausen, J.; Green, J. C.; Stelzer, F.; Baumgartner, J. *Organometallics* **2006**, *25*, 2796–2805.

(25) Sassmannshausen, J.; Track, A.; Stelzer, F. *Organometallics* **2006**, *25*, 4427–4432.

(26) Sassmannshausen, J.; Track, A.; Diaz, T. A. D. S. *Eur. J. Inorg. Chem.* **2007**, *16*, 2327–2333.

Table 2. ^1H and ^{13}C NMR Data of the Cationic Complexes **2**, **3**, and **5**

compound	^1H NMR (ppm) ^a	assgnt	^{13}C NMR (ppm) ^b	assgnt		
 <p>2 in CD_2Cl_2, $-60\text{ }^\circ\text{C}$</p>	0.44 1.37 1.60 1.66 2.49 5.78 5.85 5.95 6.06 6.31 6.77 7.44 7.67 7.74 7.74	MeB TiMe CMe ² CMe ¹ PhMe PhH ¹ Cp CpH ⁴ CpH ² CpH ¹ PhH ³ PhH ² CpH ³ CpH ¹	~ 10 23.4 20.3 29.7 37.5 68.3 106.4 112.0 114.5 118.0 119.8 121.3 126.2 141.5 142.1	CH ₃ B CC ² H ₃ PhMe CC ¹ H ₃ CCH ₃ TiCH ₃ CpC ⁴ PhC ¹ CpC ² Cp CpC ³ CpC ¹ PhC ³ PhC ⁴ PhC ²		
	^{19}F NMR ^c : $\Delta\delta(\text{m,p}) = 2.7$ ppm					
	 <p>3 in CD_2Cl_2, $-50\text{ }^\circ\text{C}$</p>	-0.68 0.99 1.52 2.15 5.32 5.60 5.83 6.68 6.81 6.85 7.22	MeB CMe ¹ CMe ² PhMe CpH ² CpH ¹ CpH ³ CpH ⁴ PhH PhH PhH ²	20.3 28.6 29.8 30.3 42.6 103.1 115.5 117.5 122.1 122.0 130.6 130.8 171.2 208.0	PhMe CC ² H ₃ CH ₃ B CC ¹ H ₃ CCH ₃ CpC ¹ Cp CpC ⁴ CpC ² PhC ³ PhC ⁴ PhC ² $\mu\text{-C-Ph}$ PhC ¹	
		 <p>5 in CD_2Cl_2, $-50\text{ }^\circ\text{C}$</p>	-0.73 0.46 1.14 2.22 6.27 6.35 6.51 6.82 6.87	$\mu\text{-Me-Ti}$ MeB TiMe PhMe Cp' Cp Cp' Cp' Ph ^{1,3} Ph ^{2,4}	~ 10 20.6 30.0 115.3 115.4 116.9 128.6 131.2	MeB PhMe TiMe Cp' Cp Cp' Cp' Ph ^{1,3} Ph ^{2,4}

OSIP.²⁷ Complete assignments of all reported cationic compounds are summarized in Table 2, and stacked plots of the aromatic region of the discussed spectra are summarized in Figure 3.

However, even gentle warming to $-50\text{ }^\circ\text{C}$ leads to a decomposition of the product with concurrent formation of methane. New peaks are growing in, suggesting the formation of a new cationic titanocene compound, which we tentatively assigned as the ISIP titanacycle $[\eta^5\text{-C}_5\text{H}_5\text{-}(\eta^5\text{-}\sigma^1\text{-C}_5\text{H}_4\text{CMe}_2\text{C}_6\text{H}_3\text{Me})\text{Ti-}\mu\text{-MeB}(\text{C}_6\text{F}_5)_3]$ (**3**) (cf. Figure 3). C–H bond activation of coordinated arenes to cationic titanium compounds has been observed before, most notably recently by Hensen for half-sandwich compounds.²⁸ Bercaw investigated the relative bond dissociation energies (BDE) of hafnocene and scandocene hydrido compounds by thermal decomposition.^{29,30} The order of relative bond dissociation energy is $\text{M}-\text{C}(\text{sp}) > \text{M}-\text{C}(\text{aryl}) > \text{M}-\text{C}(\text{sp}^3)$. For example, in the case of the hafnocene hydride $[(\eta^5\text{-C}_5\text{H}_5\text{-}(\eta^5\text{-C}_5\text{H}_4\text{CH}_2\text{C}_6\text{H}_5)\text{HfH}_2]$ the ΔBDE for (Hf–H) and (Hf–C₆H₅) is 0.8(3) kcal/mol, whereas that for (Hf–C₆H₅) and

(Hf–CH₂CH₂CH₂C₅Me₄) is 22.2(3) kcal/mol. He concluded that “the sensitivity of the transition metal–carbon bond energy to s character could be a reflection of considerable ionic ($\text{M}^{\delta+}-\text{C}^{\delta-}$) bonding, since s character at carbon increases its electronegativity.”

The proposed titanacycle thus formed should lead to a more rigid ring system, with one methyl group of the CMe₂ moiety pointing toward the “back” of the molecule, leaving the other to be more or less perpendicular to the substitute cyclopentadienyl plane (cf. DFT section for a calculated structure). We do observe a coordination of the methyl borate anion to **3** with an unusual chemical shift of the coordinated methyl group at -0.68 ppm. We observe a weak exchange with the free methyl borate (EXSY), suggesting the presence of a second titanacycle with the free coordination site probably occupied by the solvent (**4**). Unfortunately, we did not obtain clear-cut evidence for this OSIP. Solvent coordination of group 4 cationic metallocenes has been observed before, most notably by Jordan^{31–33} and us in the case of cationic zirconocene compounds.²⁵

It is known from zirconocene chemistry that cationic zirconocene compounds can be stabilized by addition of aluminum alkyls or excess starting material;^{34–36} thus, we reasoned this route might also help the stabilization of the titanocene cation. Indeed, we have demonstrated that the coordination of the neutral starting material is in some cases preferred over the coordination of the arene moiety.²⁴ Thus, the reaction of 2 equiv of **1** with 1 equiv of B(C₆F₅)₃ in CD₂Cl₂ was monitored by low-temperature NMR spectroscopy. At $-60\text{ }^\circ\text{C}$, we observe the familiar peaks for compound **2**, with the tolyl peaks being rather broad, indicating an exchange process. Additionally, peaks attributed to compound **3** can be observed. The new peak at -0.73 ppm is significant for the formation of the homodinuclear compound **5**. It is interesting to note that the formation of **5** is not the major product, nor is **5** sufficiently stable to prevent CH activation of the tolyl moiety. This is in contrast to the reaction of 2 equiv of the zirconocene compound $[(\eta^5\text{-C}_5\text{H}_4\text{SiMe}_2\text{tol})_2\text{ZrMe}_2]$ with 1 equiv of B(C₆F₅)₃ in CD₂Cl₂, which exclusively forms the homodinuclear zirconocene cation $[(\eta^5\text{-C}_5\text{H}_4\text{SiMe}_2\text{tol})_2\text{ZrMe}_2\text{-}\mu\text{-Me}]^+[\text{MeB}(\text{C}_6\text{F}_5)_3]^-$.²⁴ Mountford and Clot recently investigated in great detail the reactivity of cationic imido titanium alkyls.^{37,38} They noticed some unusual activity of the cation toward the solvent CD₂Cl₂ and $[(\eta^5\text{-C}_5\text{H}_5)_2\text{ZrMe}_2]$. In both cases, solvent and C–H bond activation was observed. The formation of adducts with AlMe₃ and ZnMe₂ was reported as well, including the solid-state structure of the AlMe₃ adduct.

Part II: DFT Calculations. An initial optimization of cation **2** from a starting structure similar to the previously reported cationic compound $[\eta^5\text{-Cp-}(\eta^5\text{-C}_5\text{H}_4\text{CH}_2\text{C}_6\text{H}_5)\text{ZrMe}]^+$ (**6**)²¹ gave structure **7a** (Figure 4). Resembling **6**, structure **7a** has a

(31) Sydora, O. L.; Kilyanek, S. M.; Jordan, R. F. *Organometallics* **2007**, *26*, 4746–4755.

(32) Stoebenau, E. J., III; Jordan, R. F. *Organometallics* **2006**, *25*, 3379–3387.

(33) Wu, F.; Dash, A. K.; Jordan, R. F. *J. Am. Chem. Soc.* **2004**, *126*, 15360–15361.

(34) Bochmann, M.; Lancaster, S. J. *Angew. Chem., Int. Ed. Engl.* **1994**, *33*, 1634–1637.

(35) Bochmann, M.; Lancaster, S. J. *Organomet. Chem.* **1995**, *497*, 55–59.

(36) Beck, S.; Prosenc, M.-H.; Brintzinger, H.-H.; Goretzki, R.; Herfert, N.; Fink, G. *J. Mol. Catal. A* **1996**, *111*, 67–79.

(37) Bolton, P. D.; Clot, E.; Cowley, A. R.; Mountford, P. *J. Am. Chem. Soc.* **2006**, *128*, 15005–15018.

(38) Bolton, P. D.; Clot, E.; Adams, N.; Dubberley, S. R.; Cowley, A. R.; Mountford, P. *Organometallics* **2006**, *25*, 2806–2825.

(27) Horton, A. D.; deWith, J.; Linden, J. v. d.; Weg, H. v. d. *Organometallics* **1996**, *15*, 2672–2674.

(28) Deckers, P. J. W.; Hensen, B. *Organometallics* **2002**, *21*, 5564–5575.

(29) Bulls, A. R.; Schaefer, W. P.; Serfas, M.; Bercaw, J. E. *Organometallics* **1987**, *6*, 1219–1226.

(30) Bulls, A. R.; Bercaw, J. E.; Manriquez, J. M.; Thompson, M. E. *Polyhedron* **1988**, *7*, 1409–1428.

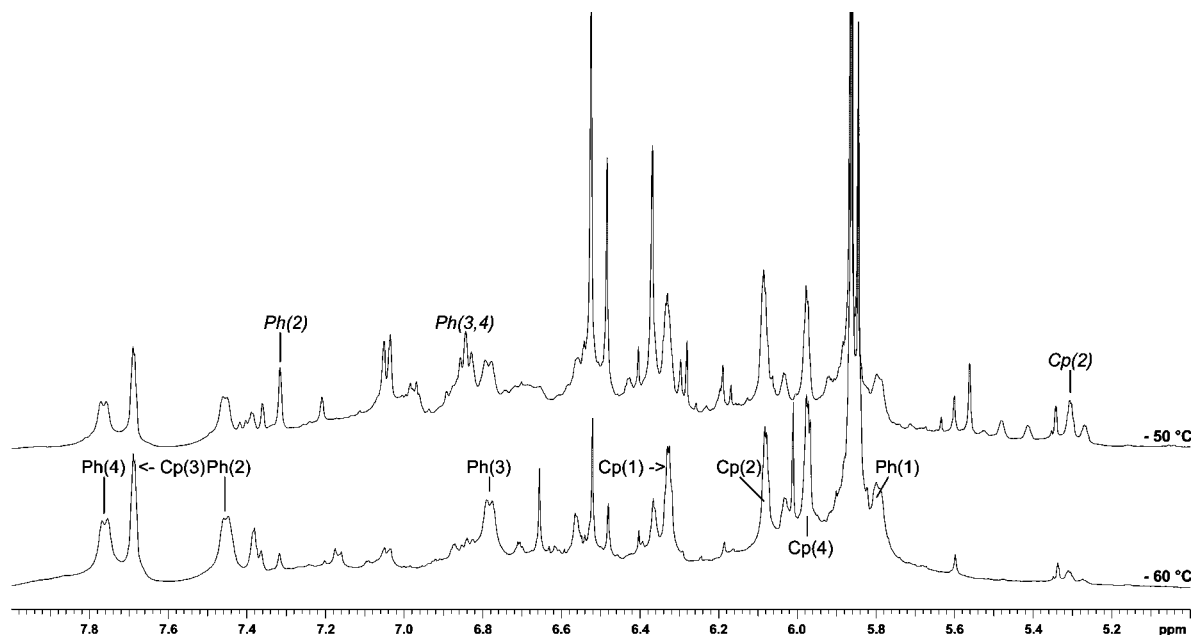


Figure 3. NMR spectra of **1** with $\text{B}(\text{C}_6\text{F}_5)_3$ in CD_2Cl_2 , aromatic region. *Italics* are used for **3**.

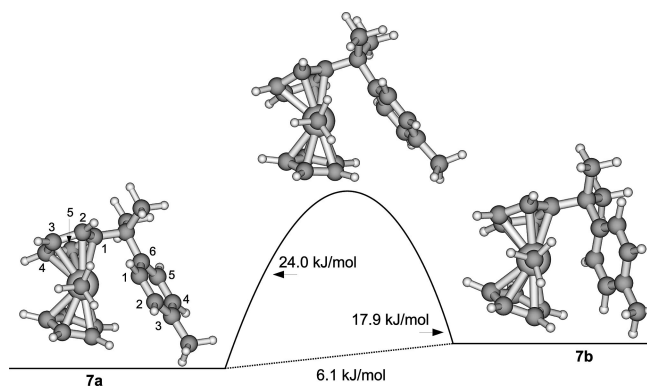


Figure 4. Stationary points and schematic potential energy surface for the phenyl rotation of cation **7**. Relative energies are at the B3LYP/ECPI level.

close contact between the Ti and one of the *ortho*-carbons of the tolyl ring (Figure 4).

The Ti–C¹ distance of 2.63 Å is larger than the sum of the van der Waals radii of Ti⁴⁺ (0.68 Å) and C⁴⁺ (0.16 Å). The hydrogen attached to C¹ of the tolyl ring is bent 9.7° out of the plane of the tolyl ring, away from the titanium. The C–H bond distance of 1.090 Å is only marginally longer than the remaining C–H bonds in the arene moiety (1.084–1.087 Å). Bader AIM analysis³⁹ corroborates a nonagostic coordination: a straight bonding path between the titanium and C¹, with a bond critical point bcp1 with an electron density $\rho(\mathbf{r}) = 0.0243$ and a Laplacian of the charge density of $\nabla^2\rho(\mathbf{r}) = -0.01909$ (Figure 5). For comparison, the values at the Ti–CH₃ bond critical point were determined to be $\rho(\mathbf{r}) = 0.0972$ and $\nabla^2\rho(\mathbf{r}) = -0.02501$. These values are slightly higher than the recently computed values for zirconocene compounds.²⁶

Further exploration of the potential energy surface revealed the presence of at least one other minimum, wherein the titanium is in close proximity to an *ortho*-carbon (**7b**, Ti–C⁵ 2.58 Å) with the attached hydrogen bent out of the Ph plane by 11.4°

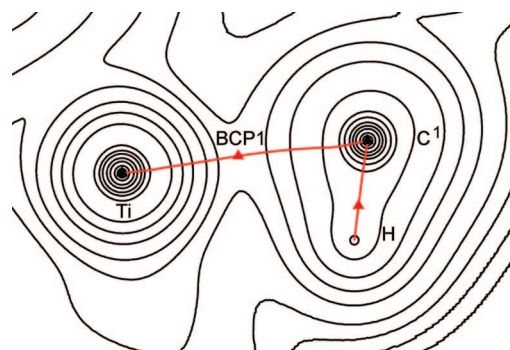
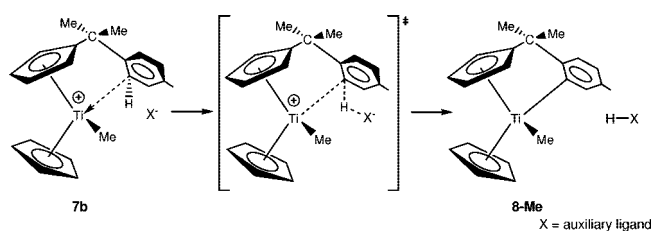


Figure 5. Bader analysis of **7a** at the B3LYP/DZVP level.

Scheme 2. Proposed Intermolecular C–H Bond Activation, Starting from 7b



(Figure 4). This second minimum is slightly higher in energy (6.1 kJ/mol) than **7a**. A transition state, **TS7**, connecting these two minima was located with a loose η^3 -coordination of the phenyl ring. The distances between titanium and C¹, C⁶, and C⁵ are 3.52, 2.95, and 3.18 Å, respectively. As the resulting barrier is only 24.0 kJ/mol (19 kJ/mol for **TS6**),²¹ scrambling between **7a** and **7b** can be expected on the NMR time scale. The Gibbs free energy of the transition state **TS7** of $\Delta G^\ddagger = 24.30$ kJ/mol indicates only a small change in entropy. As the low-temperature NMR experiment indicated the formation of methane concurrent with a change of the aromatic signals, we explored the possibility of CH activation of the arene. Two possible reaction pathways can be envisaged: the *intramolecular* C–H bond activation, where the hydrogen of the arene moiety is protonating the Ti–CH₃ bond, and the *intermolecular* C–H bond activation, where the hydrogen of the arene moiety is being

(39) Bader, R. F. W. *Atoms in Molecules: A Quantum Theory*; Clarendon Press: Oxford, UK, 1990.

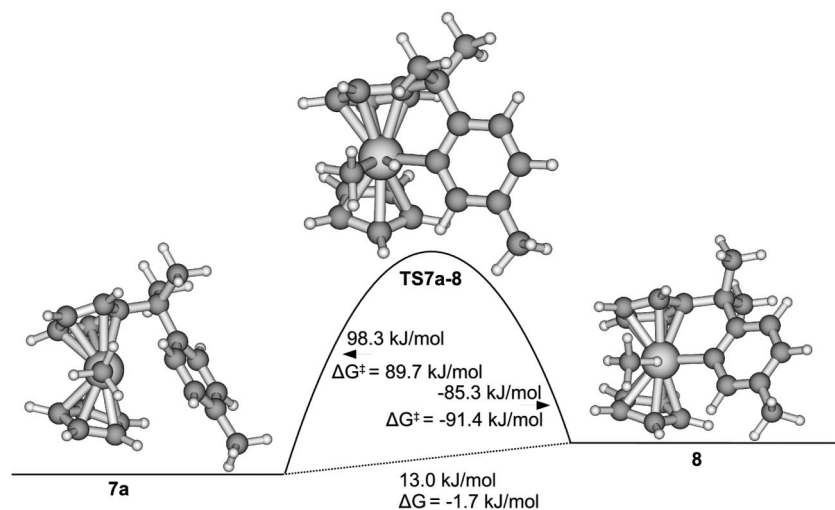


Figure 6. Stationary points and schematic potential energy surface for the CH activation of cation **7a**. Relative energies are at the B3LYP/ECP1 level.

expelled as a proton, rendering the organometallic compound neutral (Scheme 2).

We investigated only the *intramolecular* activation, as this appeared to be the most logical pathway. Starting from **7a**, we found a further minimum on the potential energy surface (**8**), with a Ti–C(arom) bond. Both compounds **7a** and **8** are connected by the transition state **TS7a-8** (Figure 6). The nature of the transition state **TS7a-8** was confirmed by frequency analysis, with one negative frequency associated with the move of the hydrogen from the arene to the methyl group, and was further corroborated by IRC analysis.

The driving force for the reaction is the release of methane. The calculated Gibbs free energy of $\Delta G^\ddagger(298.15\text{ K}) = 89.7\text{ kJ/mol}$ (88.7 kJ/mol at 213.15 K) for the transition state **TS7a-8** is significantly higher than the calculated free energy for **TS7a-b** ($\Delta G^\ddagger(298.15\text{ K}) = 24.30\text{ kJ/mol}$). As all these calculations were basically done without the influence of the solvent, i.e., in the gas phase, we were exploring the possibility of this influence on the Gibbs free energy for the activation barrier. However, including CH_2Cl_2 did not change the calculated activation energy significantly. We can therefore conclude that the *intramolecular* C–H bond activation is very unlikely to happen without *any additional* factors, like for example the influence of the anion or of catalytic amounts of $\text{B}(\text{C}_6\text{F}_5)_3$, decreasing the energy significantly. The coordination of $\text{B}(\text{C}_6\text{F}_5)_3$ to cationic zirconocene compounds has been observed before.²³ One possible *intermolecular* reaction pathway could be that the anion is close to the hydrogen of the coordinated arene carbon in **7b** and thus could abstract the proton readily (Scheme 2).

In order to corroborate our experimental NMR data, we calculated the chemical shifts for compounds **7a**, **7b**, and **8**. For the CH-activated compound **8**, we have furthermore replaced the methane molecule with an empty coordination site (**8a**), with the solvent CH_2Cl_2 (**8-sol**), with a chloride (**8-Cl**), with a methide (**8-Me**), and with the anion $[\text{MeB}(\text{C}_6\text{F}_5)_3]^-$ (**8-anion**). All calculated chemical shifts and the corresponding structure are summarized in Table 3.

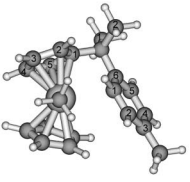
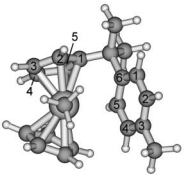
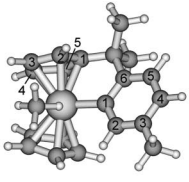
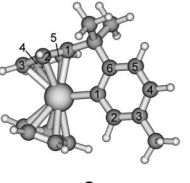
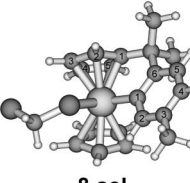
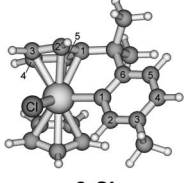
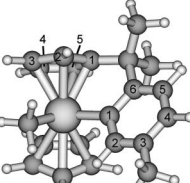
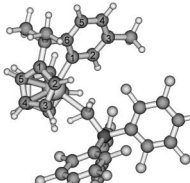
Compound **8a** was calculated as a symmetrical molecule with a mirror plane parallel to the arene moiety.⁴⁰ In order to obtain

information of the bonding mode of the Ti–C bond, we conducted a natural bonding orbital analysis (NBO). The bond with the highest second order perturbation energy (452.8 kJ/mol) is the interaction of the filled $\text{sp}^{2.76}$ hybrid orbital on carbon with the empty $\text{sd}^{14.69}$ hybrid orbital on titanium. A second bonding interaction (94.7 kJ/mol) can be found between the same carbon hybrid orbital and an empty, nearly spherical shaped $\text{sd}^{0.26}$ hybrid orbital of titanium. Together with the natural charge of this carbon of -0.548 from natural population analysis, which is similar to an sp^3 -hybridized CH_3 moiety (ranging from -0.662 to -0.693), one can conclude a highly polarized $\text{Ti}^{\delta+}\text{--C}^{\delta-}$ bond.³⁰ Interesting is the interaction of the π orbital of C–C_{ipso} (p–p) with the $p^1\text{d}^{99.99}$ of titanium (81.6 kJ/mol), which is more of donor/acceptor character. Colored plots of all discussed orbitals are available in the Supporting Information. A similar analysis was performed for **8-anion**. Here we found a significant *agostic* interaction of the H–C–B bonds with empty d orbitals of the titanium. The second-order perturbation energy was calculated between 24.4 and 43.6 kJ/mol. In particular the interaction between the CH^{66} bonding $\text{sp}^{3.04}$ orbital and the empty $\text{sp}^{0.12}\text{d}^{89.78}$ orbital of titanium was calculated to be 43.6 kJ/mol. This is also reflected by the distance between H and Ti of 2.43 Å. The second-order perturbation energy of the CH^{70} bonding $\text{sp}^{3.15}$ orbital and the CH^{71} bonding $\text{sp}^{3.49}$ orbital are 24.4 and 31.2 kJ/mol (Ti–H bond distances: 2.66 and 2.16 Å), respectively. For comparison, Marks⁴¹ reported the crystal structure of a binuclear constrained geometry titanium cation with a Ti–H(C) bonding length between 2.129 and 2.415 Å. Most interesting is an even stronger interaction (83.8 kJ/mol) of the CH^{71} (in the metallocene wedge) bonding $\text{sp}^{3.49}$ orbital with the empty $\text{sd}^{4.26}$ orbital of Ti. This is reflected not only in the shorter Ti–H bond but also in Bader analysis (Figure 7). We found a bond critical point BCP3 ($\rho(\mathbf{r}) = 0.0338$ and $\nabla^2\rho(\mathbf{r}) = -0.0323$) between the Ti–C bond, which is slightly curved toward the carbon. Interestingly, we found a BCP5 ($\rho(\mathbf{r}) = 0.01364$ and $\nabla^2\rho(\mathbf{r}) = -0.0160$) between F and C and a BCP6 ($\rho(\mathbf{r}) = 0.0147$ and $\nabla^2\rho(\mathbf{r}) = -0.0148$) between H^{71} and another F of the anion. Obviously, these interactions help in stabilizing the hyperconjugated carbon. Colored representations of the discussed orbitals are available in the Supporting Information.

(40) We have noticed that this calculated structure has a very shallow PES, and a second structure with a bent arene arrangement and lower symmetry could be obtained with the BP86 functional. As the energy difference between both structures are negligible, we did not pursue this any further.

(41) Li, H.; Li, L.; Marks, T. J.; Liable-Sands, L.; Rheingold, A. L. *J. Am. Chem. Soc.* **2003**, *125*, 10788–10789.

Table 3. Calculated Chemical Shifts of 7 and 8 at the B3LYP/NMR1 Level

						
	^1H	^{13}C	^1H	^{13}C	^1H	^{13}C
Cp	5.38	119.3	6.42	119.2	6.81	121.7
Cp ¹	-	135.2	-	139.1	-	178.9
Cp ²	5.72	107.1	5.63	107.5	5.62	113.2
Cp ³	5.81	113.9	6.23	117.4	7.47	116.3
Cp ⁴	6.28	122.4	5.06	116.2	5.48	120.2
Cp ⁵	7.36	121.6	7.10	126.9	7.60	125.9
Ph ¹	5.44	111.3	7.35	122.4	-	254.1
Ph ²	7.29	144.7	8.01	147.6	7.81	129.7
Ph ³	-	143.4	-	141.4	-	133.0
Ph ⁴	7.92	145.5	7.59	139.8	7.35	137.3
Ph ⁵	7.05	126.3	1.90	116.4	7.33	124.7
Ph ⁶	-	135.5	-	150.3	-	178.5
CMe ¹	1.54	27.7	1.27	25.8	1.82	25.5
CMe ²	1.52	19.9	1.91	21.1	0.96	26.4
TiMe	1.84	69.1	0.34	70.2	-	-
PhMe	2.49	16.4	2.38	16.6	2.37	16.5
CMe ₂	-	39.5	-	39.0	-	46.6
						
	^1H	^{13}C	^1H	^{13}C	^1H	^{13}C
Cp	7.07	126.2	6.64	119.5	5.97	114.4
Cp ¹	-	175.3	-	175.4	-	157.0
Cp ²	5.73	132.9	6.02	113.4	5.64	110.3
Cp ³	7.23	116.6	6.94	113.2	5.34	101.1
Cp ⁴	5.73	132.9	5.80	124.9	6.21	125.3
Cp ⁵	7.23	116.6	7.63	124.5	6.63	115.7
Ph ¹	-	276.1	-	243.3	-	198.7
Ph ²	8.69	133.1	7.28	129.1	7.06	136.8
Ph ³	-	132.8	-	133.1	-	132.4
Ph ⁴	7.56	138.9	7.19	135.8	6.68	126.3
Ph ⁵	7.55	125.0	7.17	124.8	6.74	123.2
Ph ⁶	-	185.3	-	176.1	-	168.6
CMe ¹	1.88	24.5	1.76	25.9	1.45	26.7
CMe ²	1.88	24.5	0.92	26.4	1.01	25.9
PhMe	2.53	16.4	2.25	16.6	2.02	17.0
CMe ₂	-	47.5	-	46.1	-	43.1
						
	^1H	^{13}C	^1H	^{13}C		
Cp	5.84	112.1	6.24	115.5		
Cp ¹	-	154.7	-	165.5		
Cp ²	5.39	106.6	6.70	118.8		
Cp ³	4.94	101.5	5.47	122.3		
Cp ⁴	6.03	118.4	5.59	103.8		
Cp ⁵	6.75	116.2	5.86	111.5		
Ph ¹	-	197.9	-	216.0		
Ph ²	6.77	133.9	7.22	131.7		
Ph ³	-	133.1	-	137.1		
Ph ⁴	6.96	126.1	6.86	129.8		
Ph ⁵	6.75	122.5	6.82	122.4		
Ph ⁶	-	169.3	-	171.1		
CMe ¹	0.97	26.7	0.95	26.2		
CMe ²	1.50	26.8	1.50	26.2		
Ti-Me	0.35	47.0	-0.53	32.3		
PhMe	2.01	17.1	2.34	17.2		
CMe ₂	-	43.4	-	44.0		

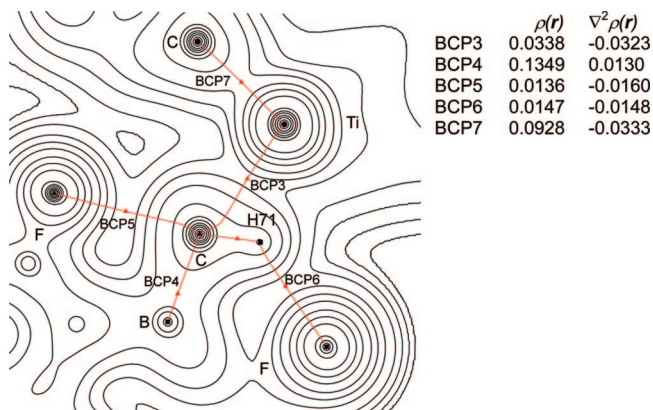


Figure 7. Bader analysis of **8-anion**, cut through the Ti–C–H⁷⁷ plane with B and F slightly out of plane, at the B3LYP/DZVP level.

Table 4. Crystallographic Data of **1a** and **1**

	1a	1
empirical formula	TiCl ₂ C ₂₀ H ₂₂	TiC ₂₂ H ₂₈
<i>M_w</i>	381.18	340.34
temperature [K]	100(2)	100(2)
size [mm]	0.36 × 0.22 × 0.18	0.38 × 0.28 × 0.22
cryst syst	monoclinic	monoclinic
space group	<i>P</i> 2(1)/ <i>n</i>	<i>P</i> 2(1)/ <i>n</i>
<i>a</i> [Å]	6.6105(2)	6.9748(2)
<i>b</i> [Å]	21.534(4)	12.204(2)
<i>c</i> [Å]	12.248(2)	21.448(4)
α [deg]	90	90
β [deg]	93.12(3)	94.90(3)
γ [deg]	90	90
<i>V</i> [Å ³]	1741(5)	1819(2)
<i>Z</i>	4	4
ρ_{calc} [g cm ⁻³]	1.454	1.243
absorp coeff [mm ⁻¹]	0.795	0.469
<i>F</i> (000)	792	728
θ range	1.91 < θ < 24.00	1.91 < θ < 24.99
no. of reflns collected/unique	10 986/2722	12 620/3196
completeness to θ [%]	99.7	99.8
no. of data/restraints/params	2722/0/211	3196/0/213
goodness of fit on <i>F</i> ²	1.11	1.04
final <i>R</i> indices [<i>I</i> > 2 σ (<i>I</i>)]	<i>R</i> 1 = 0.096, w <i>R</i> 2 = 0.199	<i>R</i> 1 = 0.079, w <i>R</i> 2 = 0.161
<i>R</i> indices (all data)	<i>R</i> 1 = 0.133, w <i>R</i> 2 = 0.220	<i>R</i> 1 = 0.090, w <i>R</i> 2 = 0.168
largest diff peak/hole [e ⁻ /Å ³]	1.01/−0.70	0.70/−0.63

The calculated chemical shifts of **8-anion** are in excellent agreement with the observed chemical shifts. In particular, the calculated high-field shift of the *MeB* of δ (ppm) −0.53, which is indicative of the coordinated anion to the metal center, is in excellent agreement with the observed chemical shift of δ (ppm) −0.68. This high-field shift is due to the magnetic anisotropy of the arene moiety in the titanacycle. Due to the observed exchange between this coordinated methyl borate and the noncoordinated methyl borate in the experiment, it is tempting to speculate about the presence of a second titanacycle in solution, probably with the free coordination site occupied by solvent (**8-sol**). However, we did not obtain any clear-cut evidence for this.

Experimental Section

All experiments were carried out under a nitrogen atmosphere using standard Schlenk techniques. Solvents were dried over sodium (toluene, low in sulfur), sodium/potassium alloy (diethyl ether, pentane), potassium (thf), and calcium hydride (dichloromethane). NMR solvents were dried over activated molecular sieves, freeze

thawed, and stored in Young's tap sealed ampules. All chemicals were purchased from Aldrich and used as received.

NMR spectra were recorded on a Varian Gemini 200 or a Varian UnityPlus 500 spectrometer and referenced to the residual protio solvent peak for ¹H. Chemical shifts are quoted in ppm relative to tetramethylsilane. ¹³C NMR spectra were referenced with the solvent peak relative to TMS and were proton decoupled using a WALTZ sequence.

Computational Details. Density functional theory calculations were carried out using the GAUSSIAN03, Revision C.02.⁴² program package, running on a Debian Etch Linux Dual-Opteron or a Dual-Xeon system, respectively. Geometries have fully been optimized without symmetry constraints, involving the functional combinations according to Becke⁴³ (hybrid) and Lee, Yang, and Parr⁴⁴ (denoted B3LYP), with the corresponding valence basis set for Ti (Stuttgart–Dresden, keyword SDD in Gaussian) and standard 6-31G* basis set⁴⁵ for C, H, F, and B (denoted as ECP1). The stationary points and transition states were characterized as minima by analytical harmonic frequency (zero or one imaginary frequency, respectively), which were used without scaling for zero-point and thermal corrections.

Magnetic shieldings σ have been evaluated for the B3LYP/ECP1 geometries using a recent implementation of the GIAO (gauge-included atomic orbitals)-DFT method,⁴⁶ involving the same B3LYP level of theory, together with the recommended IGLO basis set⁴⁷ on C, H, F, and B. For Ti, an extended Wachters basis set was used.^{48,49} This combination is denoted as NMR1. This approach with this particular combination of functionals and basis sets has proven to be quite effective for chemical shift computations for transition metal complexes.²¹ ¹H and ¹³C chemical shifts have been calculated relative to benzene as a primary reference and TMS for comparison, with absolute shieldings for benzene σ (¹H) 24.54 and σ (¹³C) 47.83 and for TMS σ (¹H) 31.73 and σ (¹³C) 177.59 with the IGLO II basis set. The values for benzene were converted into the TMS scale using the experimental δ values of benzene (7.26 and 128.5, respectively). Tables of Cartesian coordinates of all calculated structures are available as electronic Supporting Information (ESI) in *x*, *y*, *z* format. Bader and NBO5 analyses were performed using the DZVP all-electron basis set on Ti⁵⁰ and 6-31G* for C, H, F, and B. Drawings of the electron charge density plots were made using Aim2000.⁵¹ MOLDEN⁵² was used for the chemical representation of the calculated compounds, and NBO-View for the representation of the orbitals.⁵³

For the calculations including the solvent, the PCM model implemented in Gaussian03 was used, together with the UFF, and CH₂Cl₂ was chosen as a solvent. For X-ray structure analyses the crystals were mounted onto the tip of glass fibers, and data

(42) Frisch, M. J.; et al. *GAUSSIAN03, Revision C.02*; Gaussian, Inc.: Pittsburgh, PA, 2004 (see Supplementary Information).

(43) Becke, A. D. *J. Chem. Phys.* **1993**, *98*, 5648–5642.

(44) Lee, C.; Yang, W.; Parr, R. G. *Phys. Rev. B* **1988**, *37*, 785–789.

(45) Hehre, W. J.; Ditchfield, R.; Pople, J. A. *J. Chem. Phys.* **1972**, *56*, 2257–2261.

(46) Cheeseman, J. R.; Trucks, G. W.; Keith, T. A.; Frisch, M. J. *J. Chem. Phys.* **1996**, *104*, 5497–5509.

(47) Kutzelnigg, W.; Fleischer, U.; Schindler, M., *NMR Basic Principles and Progress*; Springer-Verlag: Berlin, 1990; Vol. 23, pp 165–262.

(48) Bühl, M.; Mauschick, F. T. *Magn. Reson. Chem.* **2004**, *42*, 737–744.

(49) Wachters, A. J. H. *J. Chem. Phys.* **1970**, *52*, 1033–1036.

(50) Godbout, N.; Salahub, D. R.; Andzelm, J. *Can. J. Chem.* **1992**, *70*, 560.

(51) Biegler-König, F.; Schönbohm, J.; Bayles, D. *J. Comput. Chem.* **2001**, *22*, 545–559.

(52) Schaftenaar, G.; Noordik, J. H. Molden: a pre- and post-processing program for molecular and electronic structures. *J. Comput.-Aided Mol. Des.* **2000**, *14*, 123–134.

(53) Glendening, E. D.; Badenhoop, J. K.; Reed, A. E.; Carpenter, J. E.; Bohmann, J. A.; Morales, C. M.; Weinhold, F. *NBO 5.G.*; Theoretical Chemistry Institute: University of Wisconsin, Madison, WI, 2001.

collection was performed with a Bruker-AXS SMART APEX CCD diffractometer using graphite-monochromated Mo K α radiation (0.71073 Å). The data were reduced to F_o^2 and corrected for absorption effects with SAINT⁵⁴ and SADABS,⁵⁴ respectively. The structures were solved by direct methods and refined by a full-matrix least-squares method (SHELXL97).⁵⁴ If not noted otherwise all non-hydrogen atoms were refined with anisotropic displacement parameters. All hydrogen atoms were located in calculated positions to correspond to standard bond lengths and angles. All hydrogen atoms were omitted for clarity. Crystallographic data (excluding structure factors) for the structures of compounds **1** and **2** reported in this paper have been deposited with the Cambridge Crystallographic Data Centre as supplementary publication no. CCDC 674039 (**1a**) and CCDC 674038 (**1**). Copies of the data can be obtained free of charge on application to The Director, CCDC, 12 Union Road, Cambridge CB2 1EZ, UK [fax: (internat.) +44-1223/336-033; e-mail: deposit@chemcryst.cam.ac.uk].

Preparation of $[\eta^5\text{-C}_5\text{H}_5\text{-}(\eta^5\text{-C}_5\text{H}_4\text{CMe}_2\text{C}_6\text{H}_4\text{Me})\text{TiCl}_2]$ (1a**).** The compound 4-bromotoluene (4.32 g, 25.2 mmol) was slowly added to a solution of *n*-butyllithium (10 mL, *c* = 2.5 mol/L in hexanes) in 200 mL of diethyl ether. The reaction mixture was stirred for 1 h at ambient temperature and cooled to -78°C . Next, neat dimethylfulvene (2.6 g) was added. The white suspension was slowly warmed to ambient temperature and stirred for 1 h. THF (10 mL) was added, the resulting pale yellow solution was recooled to -78°C , and $[\eta^5\text{-C}_5\text{H}_5\text{-TiCl}_3]$ (5.0 g, 25.2 mmol) was added. The dark colored solution was slowly warmed to ambient temperature and stirred for 2 days. The volatiles were removed under vacuum, and the residue was extracted into dichloromethane. Removing the volatiles under vacuum and washing the residue with a small portion of pentane yielded **1a** in pure quality. A sample for elemental analysis was recrystallized from toluene, and the so-obtained red needles were suitable for X-ray spectroscopy.

Yield: 6.0 g/62.5%/15.7 mmol. Anal. Found: C 63.06, H 5.71. $\text{C}_{20}\text{H}_{22}\text{Cl}_2\text{Ti}$ requires: C 63.02, H 5.82. ^1H NMR (CDCl_3 , 200 MHz, 20°C): δ (ppm) 1.66 (s, 6H, CCH₃); 2.42 (s, 3H, PhCH₃); 6.24 (s, 5H Cp); 6.40 (t, 2H, Cp'); 6.57 (t, 2H, Cp'); 7.06–7.08 (br, 4H, $-\text{C}_6\text{H}_4^-$). ^{13}C NMR (CDCl_3 , 50 MHz, 20°C): δ (ppm) 20.8 (PhCH₃); 29.3 (CCH₃); 40.6 (CCH₃); 119.7 (Cp'); 120.1 (Cp'); 120.4 (Cp); 126.3 (*m*-C-tolyl); 128.9 (*o*-C-tolyl); 136.0 (*i*-C-PhMe); 145.7 (*i*-C-Cp); 146.4 (*i*-C-Cp).

Preparation of $[\eta^5\text{-C}_5\text{H}_4\text{CMe}_2\text{C}_6\text{H}_4\text{Me})\text{TiMe}_2]$ (1**).** The compound **1a** (3.0 g, 7.8 mmol) was suspended in 100 mL of toluene, and methyl lithium (9.8 mL, *c* = 1.6 mol/L in diethyl ether) was slowly added at 0°C . The suspension was stirred at this temperature

for 3 h. The volatiles were removed under vacuum, and the residue was extracted into pentane (3 times with 40 mL). Red crystals suitable for X-ray analysis could be obtained by cooling the concentrated extract to -30°C .

Yield: 0.78 g/2.2 mmol/28%. Anal. Found: C 77.60, H 8.23. $\text{C}_{22}\text{H}_{28}\text{Ti}$ requires: C 77.63, H 8.29. ^1H NMR (CDCl_3 , 200 MHz, 20°C): δ (ppm) -0.05 (s, 6H TiCH₃); 1.51 (s, 6H, CCH₃); 2.35 (s, 3H, PhCH₃); 5.98 (s, 5H, Cp); 6.07 (m, 2H, Cp'); 6.12 (m, 2H, Cp'); 7.14 (s, 2H, tolyl); 7.16 (s, 2H, tolyl). ^{13}C NMR (CDCl_3 , 50 MHz, 20°C): δ (ppm) 20.8 (PhCH₃); 29.7 (CCH₃); 39.6 (CCH₃); 45.6 (TiCH₃); 111.8 (Cp'); 113.6 (Cp); 114.1 (Cp'); 126.0 (tolyl); 128.7 (tolyl).

Conclusion

The titanocene compound $[\eta^5\text{-C}_5\text{H}_5\text{-}(\eta^5\text{-C}_5\text{H}_4\text{CMe}_2\text{C}_6\text{H}_4\text{Me})\text{-TiMe}_2]$ (**1**), prepared from the titanocene dichloride precursor $[\eta^5\text{-C}_5\text{H}_5\text{-}(\eta^5\text{-C}_5\text{H}_4\text{CMe}_2\text{C}_6\text{H}_4\text{Me})\text{TiCl}_2]$ (**1a**), reacts in CD_2Cl_2 at -60°C with $\text{B}(\text{C}_6\text{F}_5)_3$ to yield the outer sphere ion pair $[\eta^5\text{-C}_5\text{H}_5\text{-}(\eta^5\text{-}\eta^1\text{-C}_5\text{H}_4\text{CMe}_2\text{C}_6\text{H}_4\text{Me})\text{TiMe}]^+$ (**2**) with a coordinated tolyl group. Warming the sample to -50°C leads to CH activation of the coordinated arene ring and the formation of the titanacycle $[\eta^5\text{-C}_5\text{H}_5\text{-}(\eta^5\text{-}\sigma^1\text{-C}_5\text{H}_4\text{CMe}_2\text{C}_6\text{H}_3\text{Me})\text{Ti-}\mu\text{-MeB}(\text{C}_6\text{F}_5)_3]$ (**3**), which is in exchange with an outer sphere ion pair $[\eta^5\text{-C}_5\text{H}_5\text{-}(\eta^5\text{-}\sigma^1\text{-C}_5\text{H}_4\text{CMe}_2\text{C}_6\text{H}_3\text{Me})\text{Ti}]^+$ (**4**), and methane. The structure of **4** could not be unambiguously assigned. Detailed computational DFT studies support the formation of **2** and **3**. As previously reported, the coordination of the arene ring in **2** can be best described as nonagostic. Bader and NBO analyses suggest the *agostic* coordination of the methyl borate to the metal center in **3**. Furthermore, the hyperconjugated carbon in the methyl borate anion is further stabilized from a nearby fluorine atom.

Acknowledgment. J.S. thanks J. C. Green, M. Bühl, and M. Flock for helpful discussions. We thank the IT department for computational resources. Financial support from the Land Steiermark, Österreich (county of Styria, Austria), is gratefully acknowledged.

Supporting Information Available: Tables of cartesian coordinates of all calculated structures, (x, y, z format), colored NBO plots and full citation of G03. This material is available free of charge via the Internet at <http://pubs.acs.org>.